# A new control allocation algorithm to improve runway centerline tracking at landing v2.3

Edouard Sadien, Clément Roos, Abderazik Birouche, Mathieu Carton, Christophe Grimault, Louis Emmanuel Romana, Michel Basset

# A new control allocation algorithm to improve runway centerline tracking at landing v2.3

**Edouard Sadien** * **Clément Roos** ** **Abderazik Birouche** ***
**Mathieu Carton** * **Christophe Grimault** * **Louis Emmanuel Romana** *
**Michel Basset** ***

* *Airbus Operations S.A.S., Toulouse, France*
*e-mail: <edouard.sadien, mathieu.carton, christophe.grimault, louis-emmanuel.romana>@airbus.com*
** *ONERA, The French Aerospace Lab, Toulouse, France*
*e-mail: clement.roos@onera.fr*
*** *IRIMAS, Université de Haute-Alsace, Mulhouse, France*
*e-mail: <abderazik.birouche, michel.basset>@uha.fr*

**Abstract:** To achieve high performance level during ground operations, the lateral dynamics of an aircraft must be controlled using all available actuators (rudder, nose wheel steering system and brakes), which gives rise to a challenging allocation problem. After an extensive literature review and evaluation of the most promising techniques, a novel and easily implementable control allocation technique is developed, which meets actuator and implementation constraints. It automatically manages the trade-off between minimizing actuator use and attaining the maximum virtual control. It is tested on a realistic on-ground aircraft model, which has been previously validated against a high-fidelity Airbus simulator.

*Keywords:* control allocation, guidance and control architecture, on-ground aircraft.

## 1. INTRODUCTION

Many airborne phases of commercial flights have been automated with the development of fly-by-wire solutions [Traverse et al. (2004)]. However, after touchdown, the motion of the aircraft is usually controlled manually by the pilot using the throttle levers, the rudder pedals, the handwheels and the brake pedals. This is especially demanding in adverse conditions such as contaminated runways and severe crosswinds. Following a study carried out by the International Civil Aviation Organization, the count of runway excursions has not decreased over the last 20 years [Eurocontrol (2013)]. The main factors, analyzed in van Es (2010), are wet/contaminated runways, crosswinds and nose wheel steering (NWS) problems. Nevertheless, automation is possible under constraining ground infrastructure and operational requirements.

Therefore, there is a strong motivation to develop enhanced control allocation algorithms able to manage multiple devices with different characteristics. But at present, solutions are rare and often only partial. Several design strategies have been proposed to control the aircraft using the NWS system only, or less frequently with the rudder as well (see *e.g.* Roos et al. (2010); Lemay et al. (2011); Looye (2007)). A lot of progress has also been made in the longitudinal energy management and control [Villaumé (2002); Duprez et al. (2004)], such as the Brake To Vacate function developed by Airbus [Villaumé and Lagaillarde (2015)]. But one of the most challenging on-ground control problems – which currently lacks a satisfactory solution – occurs at intermediate speed ($V \in [40, 80]$ knots), where the rudder and the NWS system are less efficient. The main objective is to ensure that the lateral deviation with respect to the runway centerline remains acceptable despite wind, varying runway state and comfort constraints. Achieving good performance during this worst-case scenario makes it necessary to use differential braking in addition to classical control devices (rudder and NWS system). But on the other hand, brakes should only be used sparingly to avoid a deterioration in braking performance and an increase in ground holding time for maintenance or cooling purposes.

Several control allocation techniques available in the literature (see *e.g.* Johansen and Fossen (2013); Oppenheimer et al. (2010)) can be applied to the aforementioned issue, and a thorough comparison is performed in Sadien et al. (2019). But none of them satisfies all industrial requirements, such as implementation constraints, determinism, reasonable computing power and certification aspects. In this context, a novel allocation technique is proposed in this paper, which could be implemented on board commercial aircraft in a near future. It takes advantage of the implementation ease of the pseudo-inverse approach, while smartly managing the trade-off between minimizing the use of actuators and attaining maximum virtual control.

The paper is organized as follows. The control objectives are stated in Section 2. The whole control architecture is summarized in Section 3. The emphasis is then placed on control allocation in Section 4, which recalls the most promising techniques and proposes a new algorithm. Detailed open- and closed-loop simulations are finally performed in Section 5 using the realistic aircraft model developed in Sadien et al. (2018).

## 2. CONTROL OBJECTIVES

During the rollout phase, the main objective is to ensure that the aircraft remains on the runway despite external disturbances such as wind and varying runway state. Currently implemented solutions only make use of the rudder and the NWS system. In order to use both actuators optimally, it is desirable that

they reach saturation almost simultaneously to allow efficient recovery in case of failure. Indeed, having a failed actuator at maximum deflection and the other at smaller deflection requires more time to recover, which can be critical.

Moreover, there is a need to extend the operational domain, taking into account demanding scenarios and failure cases through the smart use of differential braking. Regulations require aircraft brakes to be able to handle a rejected or aborted takeoff at any moment prior to the plane reaching a decision speed. To make this possible, the brakes should not exceed a specified temperature before engaging a takeoff, so as to avoid a subsequent performance degradation or a fire breakout in the main landing gear bays. Moreover, research has shown that the number of brake applications contributes more to carbon brake wear than the intensity of each application [Brüggemann et al. (2017)]. So the minimization of differential braking is a strong industrial requirement to reduce the likelihood of brake wear and overheating, and therefore delayed departures. This is of utmost importance after ensuring the safety of the aircraft.

## 3. CONTROL ARCHITECTURE OVERVIEW

Fig. 1 shows the whole lateral ground control architecture. An outer-loop guidance law **G** first computes the body-axis yaw rate command $r_c$ to minimize the aircraft lateral deviation despite wind disturbance $W$ and varying runway state $\bar{\mu}$. The inner-loop dynamic inversion control law **NDI** then generates a virtual yaw acceleration command $\dot{r}_{act_c}$ to be produced by the actuators via the control allocation module **CA**. The latter finally outputs the commanded actuator deflections and interacts with the longitudinal controller **L** for the brakes management.

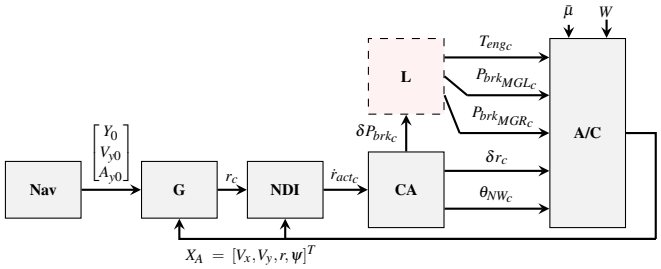


Fig. 1. Lateral ground control architecture

*Guidance Law*

The guidance law (**G block**) is given by:

$$r_c = K_y (Y_0 - Y_c) + K_{Vy} V_{y0} + K_{Ay} A_{y0} \tag{1}$$

where $Y_c$, $Y_0$, $V_{y0}$ and $A_{y0}$ denote respectively the reference lateral distance from the runway centerline (equal to zero here), the actual lateral distance, and the lateral velocity and acceleration in the runway reference system, given by the navigation system (**Nav block**). In practice, the transfer function between $Y_0$ and $Y_c$ is first computed. To do so, $V_{y0}$ and $A_{y0}$ are replaced with $sY_0$ and $s^2Y_0$ respectively, $r_c$ is replaced with the yaw rate $r$ as shown in (6), and $r$ is connected to $Y_0$ as follows:

$$s^2 Y_0 = \frac{V_x}{1+\tau_y s} r \tag{2}$$

where $V_x$ denotes the longitudinal velocity. The gains $K_y$, $K_{Vy}$ and $K_{Ay}$ are then computed by a modal approach so that the transfer between $Y_c$ and $Y_0$ is well-damped and sufficiently fast.

*Nonlinear Dynamic Inversion based Yaw Rate Control Law*

The yaw angular acceleration is the sum of a control-independent acceleration $\dot{r}_B$ and a control-dependent acceleration $\dot{r}_{act}$:

$$\dot{r} = \dot{r}_B + \dot{r}_{act} \tag{3}$$

Non-linear dynamic inversion (NDI), also known as feedback linearization (see *e.g.* [Isidori (1995)]), allows to cancel certain system dynamics and to reduce the initial control problem to the control of a simple linear system. Here, the yaw angular acceleration $\dot{r}$ is first expressed as a function of the control input $\dot{r}_{act}$, and this relationship is inverted to have $\dot{r}_{act}$ as a function of $\dot{r}$. The closed-loop dynamics are then imposed by forcing $\dot{r}$ to be equal to a desired value $\dot{r}_M$. This yields the following inverse law (**NDI block**):

$$\dot{r}_{act_c} = \dot{r}_M - \dot{r}_B \tag{4}$$

$$\dot{r}_M = k_d r_c + k_i \int (r_c - r) + k_r r \tag{5}$$

where the desired yaw rate $r_c$ is determined by the guidance law. The following transfer function between $r$ and $r_c$ is finally obtained:

$$\frac{r}{r_c} = \frac{(1+\tau_r s)\,\omega_r^2}{s^2 + 2\xi_r \omega_r s + \omega_r^2} \tag{6}$$

where the frequency $\omega_r$, the damping $\xi_r$ and the time constant $\tau_r$ depend on the gains $k_d$, $k_i$ and $k_r$. The latter are tuned so that the closed-loop system is fast and well-damped.

*Control Allocator*

The number of control effectors being greater than the number of controlled variables, an allocation algorithm (**CA block**) is required to distribute $\dot{r}_{act_c}$ among the redundant set of actuators. It produces the commanded nose-wheel and rudder deflections $\theta_{NW_c}$ and $\delta r_c$, as well as the difference $\delta P_{brk_c} = P_{brk_{MGR_c}} - P_{brk_{MGL_c}}$ between the right and left braking pressures.

*Longitudinal Controller*

The longitudinal controller (**L block**) computes the mean braking pressure $P_{brk_{COM_c}}$ and thrust command $T_{eng_c}$. The commanded left and right braking pressures are then obtained as:

$$\begin{aligned} P_{brk_{MGL_c}} &= P_{brk_{COM_c}} - 0.5\delta P_{brk_c} \\ P_{brk_{MGR_c}} &= P_{brk_{COM_c}} + 0.5\delta P_{brk_c} \end{aligned} \tag{7}$$

*The control laws have been briefly described in this section for the sake of completeness. They are not further detailed as they are out of scope of this paper, which focuses on control allocation.*

## 4. CONTROL ALLOCATION

Mathematically, a control allocator solves an underdetermined system of equations, subject to actuator physical constraints. It is fed by a vector of virtual inputs $v(t) \in \mathbb{R}^k$ (typically a number $k$ of forces and moments that equals the number of degrees of freedom to be controlled), and it computes the true control inputs $u(t) \in \mathbb{R}^m$ to be sent to the $m$ actuators, where $m > k$. In the literature (see *e.g.* Oppenheimer et al. (2010); Johansen and Fossen (2013); Fossen et al. (2008)), effector models are almost always considered linear in $u$. Thus given $v(t)$, the allocation problem reduces to the calculation of $u(t)$ such that:

$$\begin{aligned} B(t)u(t) &= v(t) \\ \text{with } \underline{u}(t) &\le u(t) \le \overline{u}(t) \end{aligned} \tag{8}$$

where $B(t) \in \mathbb{R}^{k\times m}$ is the control effectiveness matrix of rank $k$. The considered limits are the most restrictive of the rate and position limits. They are specified as:

$$\begin{aligned} \underline{u}(t) &= \max\left\{u^p_{min}, u(t-T) + T u^r_{min}\right\} \\ \overline{u}(t) &= \min\left\{u^p_{max}, u(t-T) + T u^r_{max}\right\} \end{aligned} \tag{9}$$

where:

$$\begin{aligned} u^p_{min} \le u(t) \le u^p_{max} \\ u^r_{min} \le \dot{u}(t) \le u^r_{max} \end{aligned} \tag{10}$$

and $T$ is the sample time. In the sequel, the time $t$ is omitted unless it is necessary for the understanding of the paper.

The control allocator implemented in the **CA block** receives the virtual control input $v = \dot{r}_{act_c}$ and computes the true control inputs $u$ to be sent to the actuators. Since ganging of the left and right braking systems is considered, the number of control allocator outputs reduces to $m = 3$. Moreover, the realistic on-ground aircraft model developed and validated in Sadien et al. (2018) is used in this work. This leads to the following control vector $u$ and effectiveness matrix $B$:

$$u = \begin{bmatrix} \theta_{NW_c} \\ \delta r_c \\ \delta P_{brk_c} \end{bmatrix} \tag{11}$$

$$B = \begin{bmatrix} \frac{D_{xNW} K_{y_{NW}} F_{z_{NW}}}{I_{zz}} & \frac{q_d S c Cn_{\delta r}}{I_{zz}} & \frac{D_{yMG} N_{t_{MG}} G_{brk}}{I_{zz} R_e} \end{bmatrix} \tag{12}$$

where $q_d = \frac{1}{2}\rho {V_a}^2$, $\rho$, $V_a$, $S$, $c$, $Cn_{\delta r}$ and $I_{zz}$ are the dynamic pressure, the air density, the Euclidean norm of the aerodynamic velocity, the reference surface, the mean aerodynamic chord, the yaw stability derivative due to the effect of the rudder deflection $\delta r$ and the inertia around the vertical axis of the aircraft respectively. The distances $D_{xNW}$ and $D_{yMG}$ denote the longitudinal and lateral distances between the aircraft center of gravity, and the nose and main landing gears respectively. Moreover, $N_{t_{NW}}$, $F_{z_{NW}}$ and $K_{y_{NW}}$ denote the number of tires, the normal load and the reduced lateral cornering gain of the nose wheel respectively. The normal load $F_{z_{NW}}$ is obtained by a moment balance at the main landing gears around the lateral axis of the aircraft:

$$F_{z_{NW}} = \frac{mgD_{xMG} - F_{za}\left(D_{xMG} - c\left(c_A - c_G\right)\right)}{D_{xNW} + D_{xMG}} \tag{13}$$

where $m$, $g$, $D_{xMG}$ and $F_{za} = q_d S C z_0$ denote the aircraft mass, the standard gravity, the longitudinal distance between the aircraft center of gravity and the main landing gears, and the lift force which depends on the lift stability derivative $Cz_0$ respectively. In addition, the weight and the aerodynamic effects act at points located along the fuselage axis, whose distances w.r.t. the center of gravity are $-c_G.c$ and $-c_A.c$ respectively, $c_G$ and $c_A$ being positive dimensionless coefficients. The reduced lateral cornering gain $K_{y_{NW}}$ depends on the runway state:

$$K_{y_{NW}} = \frac{K_{yMAX_{NW}}}{\frac{2}{3} + \frac{1}{3\bar{\mu}}} \tag{14}$$

where $K_{yMAX_{NW}}$ is defined for a dry runway, and the relative friction coefficient $\bar{\mu}$ is equal to 1 for dry, 0.74 for wet and 0.29 for snowy runways. Finally, $G_{brk}$ and $R_e$ are the brake gain and the main landing gear wheel rolling radius respectively.

The nonlinearities of the ground reaction forces are not considered in the computation of the control effectiveness matrix $B$ but they are taken into account indirectly by more restrictive actuators position limits:

$$u^p_{max} = -u^p_{min} = \left[L_{pNW_{CA}}\ L_{p\delta r_{CA}}\ L_{pbrk_{CA}}\right]^T \tag{15}$$

*Remark 1.* A complete set of numerical values representative of a commercial aircraft can be found in Sadien et al. (2018).

### *4.1 Control Allocation Techniques Review*

To be considered flight worthy, a control allocation technique should meet several objectives:

(1) produce smoothly varying actuator commands that do not chatter back and forth from one time step to the next,
(2) achieve all the virtual control that the actuators can produce, minimizing some kind of "control power",
(3) minimize the allocation error in some sense in case of control deficiency,
(4) meet the deterministic criteria of the certification authorities,
(5) be compatible with the existing control laws structure,
(6) require a reasonable computing power.

In Sadien et al. (2019), the 20 most promising techniques, identified from an exhaustive literature review, have been applied to the considered on-ground aircraft lateral control application. Their performance have been assessed based on 6 key performance indicators originating from Naskar et al. (2017) and from Airbus expertise in world civil aviation. The most relevant methods identified are the weighted pseudo-inverse and the daisy chaining presented in Oppenheimer et al. (2010), the linear filter from Härkegård (2003), and the dynamic control allocator from Zaccarian (2009) due to their implementation ease and small convergence time. However, all of them have drawbacks, which are summarized below.

*Weighted pseudo-inverse [Oppenheimer et al. (2010)]*: The weighting matrix is diagonal and composed of the squared position limits of the actuators, which minimizes the control power. But the maximum attainable $\dot{r}_{act_c}$ is not accessible with such a constant weighting matrix [Durham (1993)], and the classical actuators (NWS system and rudder) do not saturate simultaneously.

*Linear filter [Härkegård (2003)]*: This method provides a "soft" means to respect rate limits at the expense of position limits violation. However, for the considered benchmark, there is no added value compared to the weighted pseudo-inverse since rate limits are rarely violated. And as above, the maximum attainable $\dot{r}_{act_c}$ cannot be reached.

*Daisy chaining [Oppenheimer et al. (2010)]*: This technique requires that a hierarchy be established between the control effectors, which are separated into different groups. In the benchmark, the first group consists of the classical actuators, and the second one of the brakes. Allocation within the first group is done using the pseudo-inverse method and differential braking is not minimized, since it is used as soon as one classical actuator saturates. A way to address this issue could be to send the overflow of $\dot{r}_{act_c}$ to the other actuator of the first group before using the second group. But the classical actuators would still not saturate simultaneously, which is not desirable.

*Dynamic control allocator [Zaccarian (2009)]*: When implemented on a digital system, there is a strong limit in the dynamic allocation speed to ensure stability. Therefore, the initial allocation should not be too far from the optimal solution, which is already an allocation problem in itself.

With reference to Section 2, the main objective is to ensure the aircraft safety through the realization of the virtual control input $\dot{r}_{act_c}$, while minimizing the use of differential braking. But as highlighted above, most existing techniques do not consider the latter objective at all. Only the daisy chaining reduces braking to some extent as the brakes are in the secondary group. Nevertheless, it does not allow the simultaneous saturation of the classical actuators. *Therefore, a new control allocation algorithm should be developed to address these issues.*

### 4.2 Proposed Control Allocation Technique

The Dynamic Weighting Control Allocator (DWCA), depicted in Fig. 2, is a pseudo-dynamical control allocation technique which automatically manages the trade-off between two antagonistic objectives: minimizing the control effort and attaining the maximum virtual control, for the 1-dimension case, *i.e.* $v \in \mathbb{R}$. Moreover, it meets the specifications given in Section 2 and respects various practical requirements such as limited computational power and implementation constraints. It also allows the consideration of actuator dynamics.

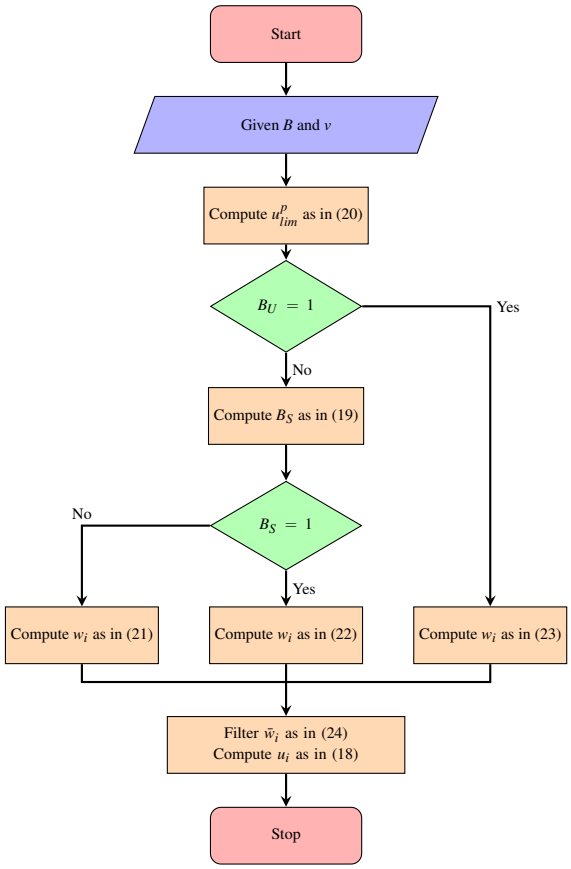


Fig. 2. Flowchart of the proposed allocation method

The DWCA requires that the $m$ actuators be grouped as "primary" or "secondary". In the *nominal mode*, actuators from the primary group are first used up to their maximum capability. They are used according to their relative efficiency and reach saturation at the same time, which is not possible with *daisy chaining*. Only then are the actuators from the secondary group used. The DWCA also presents an *unrestricted mode* activated by the boolean $B_U$, which considers all available actuators as primary. This mode may be triggered for instance according to the lateral deviation, the orientation of the aircraft and the runway state.

The following unconstrained optimization problem is solved:

$$\arg\min_{u\in\mathbb{R}^m} \frac{1}{2} u^T W^{-1} u \text{ subject to } Bu = v \tag{16}$$

where $W \in \mathbb{R}^{m\times m} = \text{diag}(\bar{w}_1, \ldots, \bar{w}_m)$ is a weighting matrix, $B = [b_1 \ldots b_m] \in \mathbb{R}^{1\times m}$ and $v \in \mathbb{R}$. The general solution is given by:

$$u = WB^T(BWB^T)^{-1}v \tag{17}$$

The commanded deflection for the $i^{th}$ actuator is then given by:

$$u_i = \text{sat}_{[u^p_{min},\, u^p_{max}]}\left(\frac{b_i \bar{w}_i}{\sum_{i=1}^m b_i^2 \bar{w}_i} v\right) \tag{18}$$

where $b_i$ is the efficiency of the $i^{th}$ actuator. The saturation operator in equation (18) is defined such that $\text{sat}_{[F_1,\, F_2]}(x) = x$ if $F_1 \le x \le F_2$, $\text{sat}_{[F_1,F_2]}(x) = F_1$ if $x < F_1$ and $\text{sat}_{[F_1,F_2]}(x) = F_2$ if $x > F_2$.

Consider now the first $n$ and the last $l$ actuators, such that $n + l = m$, as part of the primary and secondary groups respectively. While the unrestricted mode is not activated ($B_U = 0$), the use of the secondary group is triggered by the boolean $B_S$ when the virtual command $v$ cannot be realized using exclusively the primary group:

$$B_S = \begin{cases} 1 & \text{if} \quad |v| - \eta_{DWCA} \sum_{j=1}^{n} \left(|b_j| u^p_{lim_j}\right) > 0 \\ 0 & \text{otherwise} \end{cases} \tag{19}$$

The efficiency $\eta_{DWCA}$ of the control allocator is typically set between 0.9 and 1, so that the secondary actuators begin to be used slightly before all actuators from the primary group reach saturation, allowing some kind of "phase advance". The effective limit $u^p_{lim_i}$ of each actuator is given by:

$$u^p_{lim_i} = \begin{cases} |u^p_{max_i}| & \text{if} \quad b_i \cdot v \ge 0 \\ |u^p_{min_i}| & \text{otherwise} \end{cases} \tag{20}$$

In the *nominal mode*, when the use of the second group is not required ($B_S = 0$), the weighting parameters are calculated as:

$$w_{i\in\{1,\ldots,n\}}(t) = {u^p_{lim_i}}^2 + \left(\frac{1}{|b_i|} - u^p_{lim_i}\right)|u_i(t-T)| \tag{21a}$$

$$w_{i\in\{n+1,\ldots,m\}}(t) = 0 \tag{21b}$$

The weights of the secondary actuators are set to zero in (21b). Those of the primary actuators are defined as the sum of two terms in (21a): the control power minimization term ${u^p_{lim_i}}^2$ and the maximum virtual control reaching term $\frac{1}{|b_i|} - u^p_{lim_i}$. The trade-off between these two antagonist terms depends on the commanded actuator deflection at the previous time step $u_i(t-T)$. When $|u_i(t-T)|$ is small, $w_i(t) \approx {u^p_{lim_i}}^2$ and control power is minimized. But when $|u_i(t-T)|$ is close to $u^p_{lim_i}$, $w_i(t) \approx \frac{u^p_{lim_i}}{|b_i|}$ which ensures that all primary actuators reach saturation at the same time.

When the use of the secondary actuators is deemed necessary ($B_S = 1$), the weighting parameters are given by:

$$w_{i\in\{1,\ldots,n\}}(t) = \frac{u^p_{lim_i}}{|b_i|} \tag{22a}$$

$$w_{i\in\{n+1,\ldots,m\}}(t) = \frac{u^p_{lim_i}}{|b_i|} \min\left(1, \frac{|v| - \eta_{DWCA} \sum_{j=1}^{n} \left(|b_j| u^p_{lim_j}\right)}{\sum_{l=n+1}^{m} \left(|b_l| u^p_{lim_l}\right)}\right) \tag{22b}$$

The primary actuators are set to their maximum deflection in (22a). The secondary ones are set to the minimum required deflection in (22b), with an upper bound equal to their position limits.

In the *unrestricted mode* ($B_U = 1$), the weighting parameter of each actuator is given by:

$$w_{i\in\{1,\ldots,m\}}(t) = {u^p_{lim_i}}^2 + \left(\frac{1}{|b_i|} - u^p_{lim_i}\right)|u_i(t-T)| \tag{23}$$

In this case, all actuators are used the same way to manage the trade-off between minimizing control power and attaining the maximum virtual control.

Before computing the commanded deflections (18), the dynamics of each actuator is catered for by filtering the corresponding tuning parameter $w_i$ from (21)-(23) through a first order filter of time constant $\tau_i$ equal to that of the $i^{th}$ actuator:

$$\bar{w}_i(t) = \frac{1}{1+\tau_i s} w_i(t) \tag{24}$$

## 5. RESULTS AND ANALYSIS

The effectiveness of the DWCA is assessed through open- and closed-loop simulations with the control laws described in Section 3. The method is also compared to the most promising technique in the literature, namely daisy chaining.

### *5.1 Open-loop Evaluation*

The control allocation techniques identified in Section 4.1 and the DWCA are first compared on 3 scenarios corresponding to realistic $\dot{r}_{act_c}$ profiles which can be realized using (i) the conventional actuators only, (ii) all actuators and (iii) which cannot be realized with all actuators at their position limits. The indicators, in decreasing order of importance, used for comparison are:

- *Percentage of unrealized virtual control*: percentage of time during which $|Bu - v| > \varepsilon$ ($10^{-5}$ here).
- *Percentage of differential braking*: ratio $\delta P$ of the normalized consumption of differential braking to the sum of the normalized consumption of each actuator,
- *Integral of squared error*: integral of the squared difference between the commanded and the realized yaw accelerations $\dot{r}_{act_c}$ and $\dot{r}_{act}$ (with actuator dynamics considered),
- *Normalized consumption*: sum of the normalized consumption of each actuator, defined as the integral of the ratio of the actuator deflection to its maximum position,

| Method | % Unrealized virtual control | % $\delta P$ | Integral of squared error [$\times 10^{-3}$ deg/s$^3$] | Normalized consumption |
|---|---|---|---|---|
| Weighted pseudo-inverse | 7 | 19 | 3.1 | 42.4 |
| Linear filter | 7 | 19 | 3.1 | 42.4 |
| Daisy chaining | 8 | 9 | **1.8** | **41.1** |
| Dynamic control allocator | 37 | 11 | 11.5 | 126.4 |
| **Dynamic weighting control allocator** | 7 | **5** | 2.5 | 42.2 |

Table 1. Open-loop synthetic results

Virtual control realization and differential braking minimization being the main objectives, it can be observed from Table 1 that daisy chaining is the most efficient of the existing techniques. However, as discussed in Section 4.1, it does not present the best results in the realization of the virtual control due to the fact that it starts using differential braking although both conventional actuators are not saturated. Moreover, it uses almost twice as much differential braking as the DWCA. On the other hand, it has the minimum integral squared error as it uses more differential braking, which is the fastest actuator. In addition, the lowest normalized consumption result is explained by the fact that it has some more unrealized virtual control compared to the other methods. Based on the most important criteria, *the best open-loop results are obtained with the DWCA.*

### *5.2 Closed-loop Evaluation*

The DWCA and the daisy chaining are now compared in closed-loop under similar conditions. The aircraft is initialized at 120 knots with a lateral deviation of 8 m. It is aligned with the runway centerline on a dry runway and stopped when its speed reaches 20 knots. A constant tail wind of 15 knots and a lateral turbulence, using white noise and reaching a peak of 43 knots, is used, as illustrated in Fig. 4. The longitudinal distance $X_G$ is arbitrarily set to zero at the beginning of the simulation. The unrestricted mode is not activated so as to show the efficiency of the DWCA in reducing the use of the brakes. In practice, when the unrestricted mode is activated, the aircraft reaches the runway centerline faster with the DWCA than with daisy chaining with comparable use of the brakes. However, due to space constraints, the corresponding trajectories are not shown.

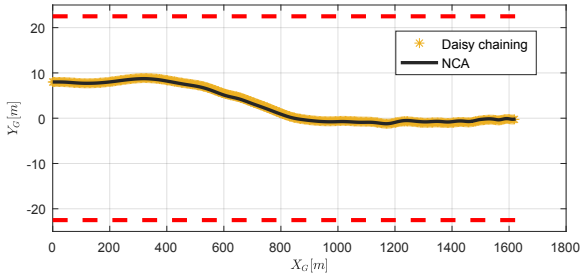


Fig. 3. Trajectory and runway limits (in dashed red)

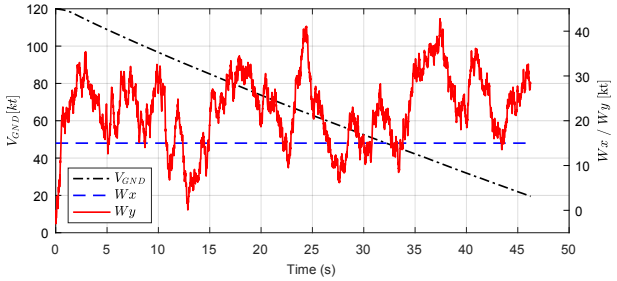


Fig. 4. Ground speed $V_{GND}$ and wind profiles

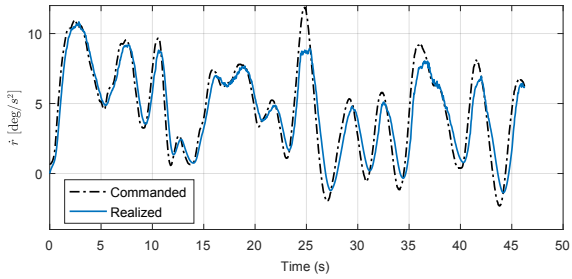


Fig. 5. Commanded and realized virtual controls for DWCA

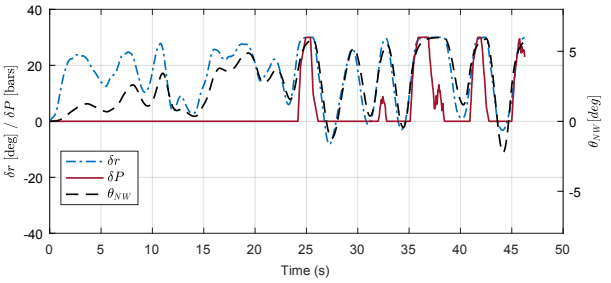


Fig. 6. Actuator deflections for DWCA

Both control allocators maintain the aircraft on the runway with a negligible difference in trajectory, as shown in Fig. 3. The commanded and the realized virtual controls for the DWCA are shown in Fig. 5. The realized one lags behind the commanded one due to the actuator dynamics. It can be noticed that at 25 s and 37 s, the command is not realized as all 3 actuators are

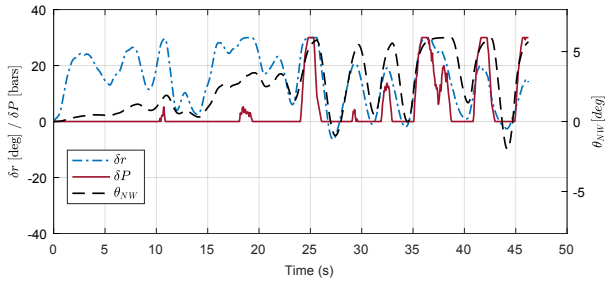


Fig. 7. Actuator deflections for daisy chaining

saturated, as shown in Fig. 6. For daisy chaining (not shown here), a similar trend is observed where the virtual control is not realized at the same moments as for the DWCA. It is very important to note that daisy chaining uses more differential braking although the NWS has not reached saturation, as it can be seen by comparing Fig. 6 and 7. Globally, daisy chaining does not minimize the use of the brakes and uses 14% more differential braking than the DWCA. It can be concluded that *the DWCA outperforms other studied algorithms on the considered application.*

## 6. CONCLUSION

In this paper, a novel methodology is proposed to solve the control allocation problem for the yaw control of an on-ground aircraft. However, the DWCA application domain is much wider and the proposed algorithm is applicable to any axis of the general vehicle control problem (aerial, space, automotive, submarine, ...). The objectives are to ensure the safety of the aircraft while minimizing the use of the brakes which is a strong industrial requirement. The proposed method intelligently manages the compromise between the realization of the command and the minimization of the control power. Moreover, it meets the aircraft manufacturer and certification authorities requirements. In contrast to daisy chaining, it ensures that the conventional actuators come to saturation at the same time, which increases the fault recovery capability, and it also takes into account actuator dynamics. The resulting algorithm has an unrestricted mode where all available actuators are used as effectively as possible. The open- and closed-loop simulation results show the effectiveness of the proposed method in comparison with several other allocation strategies. Under a difficult rollout maneuver, the proposed algorithm uses 14% less differential braking than the most efficient existing method so far. Future work will be dedicated to better efficiency estimation, for instance better estimation of the efficiency of the ground effectors with the development of a runway state estimator.

## ACKNOWLEDGEMENTS

This research is supported by Airbus Operations S.A.S., the National Association of Research and Technology (ANRT) and the French Ministry of Higher Education, Research and Innovation under the *CIFRE* contract number 2016/1058.

## REFERENCES

Brüggemann, K., Cheray, B., and Romana, L.E. (2017). Brake wear reduction apparatus. JUSTIA Patents. Patent number 20180079402. https://patents.justia.com/patent/20180079402.

Duprez, J., Mora-Camino, F., and Villaumé, F. (2004). Control of the aircraft-on-ground lateral motion during low speed roll and manoeuvers. In *Proceedings of the IEEE Aerospace Conference*, 2656 – 2666. Big Sky, U.S.A.

Durham, W.C. (1993). Constrained control allocation. *Journal of Guidance, Control and Dynamics*, 16(4), 717 – 725.

Eurocontrol (2013). European action plan for the prevention of runway excursions edition 1.0. Technical report, Eurocontrol.

Fossen, T.I., Johansen, T.A., and Perez, T. (2008). Chapter 7: A survey of control allocation methods for underwater vehicles. In A.V. Inzartsev (ed.), *Underwater Vehicles*, 109 – 128. InTech.

Härkegård, O. (2003). *Backstepping and Control Allocation with Applications to Flight Control*. Ph.D. thesis, Linköping University, Linköping, Sweden.

Isidori, A. (1995). *Nonlinear Control Systems*. Springer.

Johansen, T.A. and Fossen, T.I. (2013). Control allocation – A survey. *Automatica*, 49(5), 1087 – 1103.

Lemay, D., Chamaillard, Y., Basset, M., and Garcia, J.P. (2011). Gain-scheduled yaw control for aircraft ground taxiing. In *Proceedings of the 18th IFAC World Congress*, 12970 – 12975. Milan, Italy.

Looye, G. (2007). Chapter 8: Rapid prototyping using inversion-based control and object-oriented modelling. In D. Bates and M. Hagström (eds.), *Nonlinear Analysis and Synthesis Techniques for Aircraft Control*, 147 – 173. Lecture Notes in Control and Information Sciences, vol. 365.

Naskar, A.K., Patra, S., and Sen, S. (2017). New control allocation algorithms in fixed point framework for overactuated systems with actuator saturation. *Int. Journal of Control*, 90(2), 348 – 356.

Oppenheimer, M.W., Doman, D.B., and Bolender, M.A. (2010). Chapter 8: Control allocation. In W.S. Levine (ed.), *The Control Handbook, Control System Applications (Second Edition)*, 1 – 24. CRC Press.

Roos, C., Biannic, J.M., Tarbouriech, S., Prieur, C., and Jeanneau, M. (2010). On-ground aircraft control design using a parameter-varying anti-windup approach. *Aerospace Science and Technology*, 14(7), 459 – 471.

Sadien, E., Roos, C., Birouche, A., Carton, M., Grimault, C., Romana, L.E., and Basset, M. (2019). A detailed comparison of control allocation techniques on a realistic on-ground aircraft benchmark. In *Proceedings of the American Control Conference*. Philadelphia, U.S.A.

Sadien, E., Roos, C., Birouche, A., Grimault, C., Romana, L.E., Boada-Bauxell, J., and Basset, M. (2018). Control design oriented modeling of an on-ground aircraft. In *Proceedings of the 2018 European Control Conference*, 2757 – 2762. Limassol, Cyprus.

Traverse, P., Lacaze, I., and Souyris, J. (2004). Airbus fly-by-wire: A total approach to dependability. In *Proceedings of the 18th IFIP World Computer Congress*, 191 – 212. Toulouse, France.

van Es, G.W.H. (2010). A study of runway excursions from a european perspective. Technical Report NLR-CR-2010-259, Eurocontrol.

Villaumé, F. (2002). *Contribution à la commande des systèmes complexes : Application à l'automatisation du pilotage au sol des avions de transport*. Ph.D. thesis, Université Toulouse III - Paul Sabatier, Toulouse, France.

Villaumé, F. and Lagaillarde, T. (2015). Fast: Runway Overrun Prevention System (ROPS). Technical Report 55, Airbus, https://www.airbus.com/content/dam/corporate-topics/publications/fast/Airbus-FAST55.pdf.

Zaccarian, L. (2009). Dynamic allocation for input redundant control systems. *Automatica*, 45(6), 1431 – 1438.